CORELESS OPEN-LOOP CURRENT TRANSDUCERS
BASED ON HALL EFFECT SENSOR CSA-1V

Marjan Blagojević[1], Uglješa Jovanović[2], Igor Jovanović[2], Dragan Mančić[2], Radivoje S. Popović[3]

[1]IRC Sentronis AD, Niš, Serbia
[2]University of Niš, Faculty of Electronic Engineering, Niš, Serbia
[3]EPFL - Swiss Federal Institute of Technology, Lausanne, and SENIS AG, Zug, Switzerland

Abstract. *The paper provides an overview of coreless open-loop current transducers based on Hall effect sensor CSA-1V. Depending on the implementation method and current range, the presented transducers are divided in the four groups. The transducers are capable to measure AC and DC currents ranging from several tens of miliamperes up to several hundreds of amperes. Methods for resolving issues with the skin effect and stray magnetic fields are also presented including the experimental test results. Some of these methods are novelty and have never been presented in literature.*

Key words: *current measurement, current transducer, Hall effect sensor, CSA-1V*

1. INTRODUCTION

Hall effect refers to the voltage that appears on a conducting material when an electric current flowing through the conductor is influenced by a magnetic field [1], [2]. Hall effect is illustrated in Fig. 1, where the current I (flowing through the Hall sensor in the direction shown in Fig. 1) is deflected due to the magnetic flux density B, and thereby generates the voltage V_H.
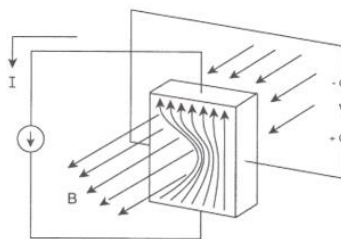
Fig. 1 Operation principle of a Hall effect sensor.

The equation which describes the output voltage of the Hall effect sensor is:

$$V_H = K_H \cdot I \cdot B \tag{1}$$

whereas K_H is coefficient which defines the sensitivity of the sensor.

Thanks to the advantages they provide, current transducers based on Hall effect sensors are used in various applications [2]. Hall effect sensors are suitable for current measurement due to their small sizes, low prices, good linearity, galvanic isolation, high bandwidth, good accuracy and the ability to measure DC current rather than only AC current [3], [4]. They can be employed to measure currents ranging from several microamperes up to several thousands of amperes.

The distribution of current density in a conductor with a rectangular cross section and equivalent schematic of this conductor are shown in Fig. 2, where each color of resistor in the schematic matches the corresponding area of a rectangular conductor. Due to the skin effect, the higher the frequency the less current flows through the resistor R_4 and more through the resistor R_1, i.e. the less current flows through the middle of the conductor and more near the outer edges [5], [6]. Current redistribution in a rectangular conductor is important factor in current measurement applications.
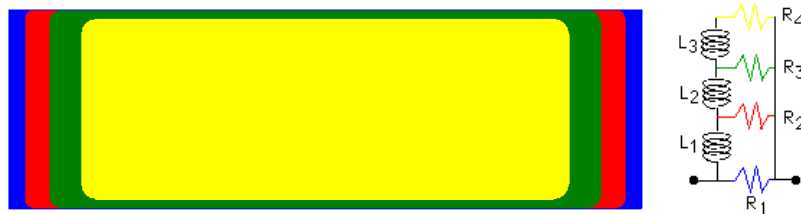
Fig. 2 Distribution of current density and equivalent schematic of a flat conductor.

The skin effect within massive rectangular conductors may become noticeable at very low frequencies in the order of several tens of Hz. The redistribution of current density results in the redistribution of the measured magnetic flux density which deteriorates frequency and phase responses of current transducers. Phase response of a current transducer is very important in applications for electric energy measurements (for instance, good current transformers have a phase shift less than 1°).

Immunity to stray magnetic fields is an important feature of current transducers based on Hall effect sensors because they can induce a false reading and measurement errors.

This paper provides an overview of current transducers based on a Hall effect sensor CSA-1V divided in the four groups. The first group works in the similar way as pickup coils and measures current in a PCB traced conductor or in a wire. The second group is based on miniature bus bars and can measure currents up to several tens of amperes. Thanks to the magnetic field increase using multi-turn coils, the third group can measure very low currents in the range of miliamperes. The fourth group is based on bus bars and it is designed for high current applications.

The major features of the transducers, the issues that arise with current measurement and the methods to overcome them are also presented in this paper. Special attention was paid to methods for resolving issues with the skin effect and stray magnetic fields.

Some of the presented solutions for frequency response improvement are novelty and, according to the knowledge of this paper authors, have never been presented in the literature.

2. HALL DEVICE CSA-1V

CSA-1V is an integrated Hall effect single-axis magnetic field sensor designed for non-contact measurement of electric current.

The device is manufactured using a standard CMOS technology with an additional Sentron's patented ferromagnetic layer called Integrated Magnetic Concentrator (IMC) [7], [8] and it incorporates the spinning current technique. Thanks to that, compared to the conventional Hall effect sensors, the CSA-1V provides a magnetic gain contributing to a greater magnetic sensitivity, a lower magnetic offset and a lower magnetic noise [9], [10].

The device is packed in a standard SOIC-8 case (see Fig. 3) which provides a good isolation (up to 600 V) for applications with current conductor traced on a printed circuit board (PCB) [9].
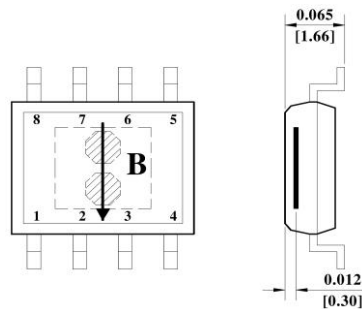
Fig. 3 Direction of the sensitivity vector and location of the sensing element [10].

The sensing element of the CSA-1V is located approximately 0.3 mm below the top surface of SOIC-8 case as illustrated in Fig. 3.

Consequence of uncontrollability of the IMC process is that CSA-1Vs will usually not have the specifications rated in the datasheet [9]. For this reason, during the manufacturing process, the calibration procedure is introduced using the certain number of specifically designated memory cells [11]. The calibration memory cells are manufactured in "zener zapping" technology and can be programed only once [12], [13]. The calibration procedure of CSA-1Vs is well presented in papers [11], [13].

3. PICKUP HALL EFFECT CURRENT TRANSDUCERS

A current transducer operating on the similar principle as a pickup coil can be realized using Hall effect sensors. In these transducers, instead of a pickup coil, the CSA-1V is employed to sense a magnetic field generated by a current carrying conductor and convert it to a voltage proportional to that field. This can be performed either by employing the CSA-1V to measure current in an adjacent wire or in a PCB traced conductor below the CSA-1V as shown in Fig. 4 [10].
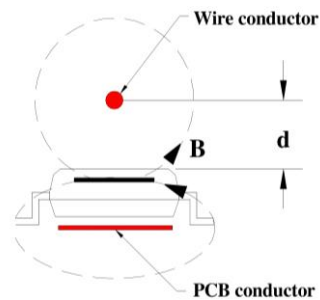
Fig. 4 Shape and direction of magnetic field from two different conductor types [10].

The CSA-1V differential output voltage for a current carrying circular conductor (wire) located on top of the sensor can be approximated with the following equation [10]:

$$V_{outdiff} \approx \frac{0.060 \cdot I}{d + 0.3} \tag{2}$$

whereas d is a distance between the CSA-1V top surface and a center of a wire given in milimeters (see Fig. 4) and I is current applied in a wire.

The application of the CSA-1V measuring current in a current carrying wire is shown in Fig. 5. If placed too close to the CSA-1V, high current carrying wire can saturate the CSA-1V. Therefore, the limits for electrical and magnetic saturation must be taken into the account.
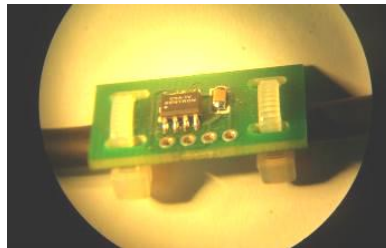
Fig. 5 Application of the CSA-1V measuring current in a current carrying wire.

The CSA-1V differential output voltage for a flat PCB conductor traced directly below the CSA-1V can be approximated with the following equation [10]:

$$V_{outdiff} \approx 40 \cdot I \tag{3}$$

whereas I is current applied in a PCB traced conductor assumed to be roughly 3.2 mm wide.

The sizing of the PCB trace needs to take in account the current handling capability and the total power dissipation. For this reason, the PCB trace needs to be thick enough and wide enough to handle designated nominal current continuously. Using a single PCB traced conductor, currents up to 10 A can be measured. The applications of the CSA-1V measuring current in the PCB traced conductor (see Fig. 6) are presented in paper [14] while the thermal analysis performed using the thermal imaging camera is presented in paper [15].
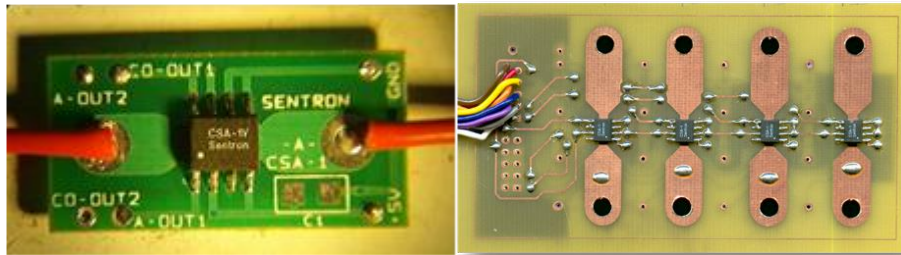
Fig. 6 Applications of the CSA-1V measuring current in the PCB trace [14], [15].

Applications shown in Fig. 6 are implemented in photovoltaic power plant for DC current measurement of photovoltaic modules [14].

3.1. Transducer with the magnetic shield

The CSA-1V can detect any surrounding stray magnetic field which is in the direction of sensitivity (across the chip) which may cause interference and disturb the measurement accuracy. The solution to this issue is to shield the CSA-1V by mounting a small (roughly 1 cm^2 x 0.5 mm) ferromagnetic plate on the opposite side of a PCB from the one to which the CSA-1V is soldered as shown in Fig. 7 [10]. The plate can be made out of Mu-metal since it has high permeability at low field strengths and low remanence field.
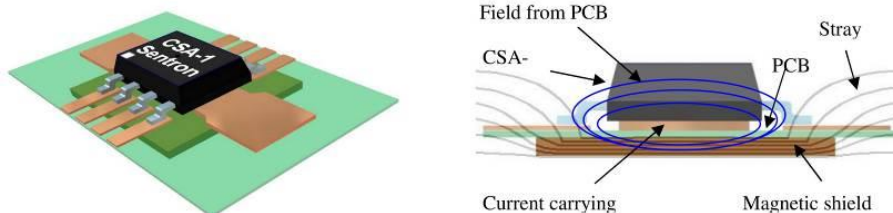
Fig. 7 Shielding the CSA-1V from stray fields [10].

The ferromagnetic shield has double effect:

1. It concentrates the flux around the trace thus shortening the field lines that go through the air almost by double. In this way the magnetic resistance is reduced by double which ultimately contributes to higher induction and greater output signal (by 30%−50%).

2. It serves as the concentrator for stray fields at the same time deflecting them from the CSA-1V as shown in Fig. 7.

3.2. Anti-differential configuration of Hall effect sensors

Measurement error produced by stray fields can be also minimized by implementing two Hall effect sensors in the anti-differential configuration shown in Fig. 8.
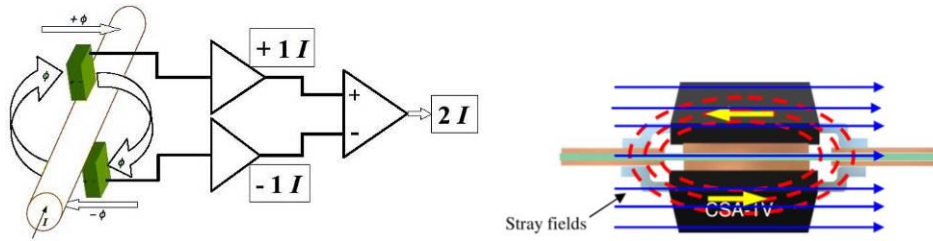
Fig. 8 Anti-differential configuration of Hall effect sensors [10].

Implementation of this method cancels common mode magnetic fields while the output signal is doubled [10] as per following equations:

$$U_1 = S \cdot (B + B_S) \tag{4}$$

$$U_2 = S \cdot (B - B_S) \tag{5}$$

$$U_1 + U_2 = 2 \cdot S \cdot B \tag{6}$$

whereas B is the measured magnetic field, B_S is the common mode magnetic field and S is the sensor sensitivity. This method works perfectly with homogenous stray fields. Since the field gradient decreases as a function of distance, if the surrounding nonhomogeneous stray fields are relatively distant from the transducer they can be considered as homogeneous.

In this way, the useful signal is doubled while the noise is $\sqrt{2}$ greater, i.e. the signal to noise ratio is $\sqrt{2}$ times better. Application of anti-differential configuration of the CSA-1Vs on the massive oval conductor is shown in Fig. 9.
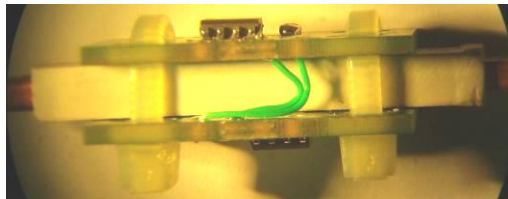
Fig. 9 Application of anti-differential configuration on the massive oval conductor.

4. MINIATURE BUS BAR CURRENT TRANSDUCERS

Currents greater than 10 A can be measured using the CSA-1V by conducting current throughout a properly shaped copper miniature bus bar (MBB) placed above the CSA-1V as illustrated in Fig. 10.

Fig. 10 Copper MBB placed above the CSA-1V.

Sizing of the MBB and the distance from the CSA-1V are dependent on the desired current handling capability. The closer the MBB to the CSA-1V, the more accurate readings will be obtained but the limits of electrical and magnetic saturation need to be taken into the account. The approximate CSA-1V differential output voltage can be obtained by the following equation:

$$V_{outdiff} \approx \frac{40 \cdot I}{(d + 0.3)} \tag{7}$$

whereas d is the distance between the MBB center and the CSA-1V top surface given in millimeters and I is current applied in the MBB.

The method illustrated in Fig. 10 can easily be implemented by soldering a MBB on to a PCB above the CSA-1V as shown in Fig. 11 [10].
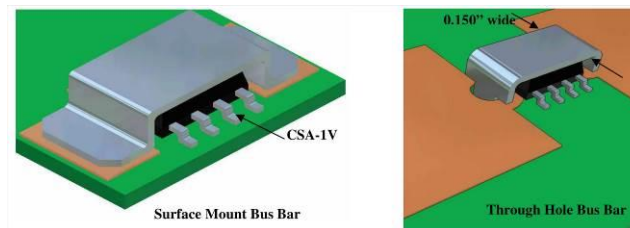
Fig. 11 Application of a MBB and a PCB trace [10].

When a noncircular MBBs are employed in the application illustrated in Fig. 11, it is necessary to take into the account frequency dependence of transducer's sensitivity because the skin effect forces high frequency current to flow along the outer edges of the MBB thus changing the magnetic flux density at the site of the CSA-1V. Consequently, the frequency response deteriorates.

The solution to this issue is to split a rectangular MBB into two parallel branches by drilling a hole in the middle of a MBB as illustrated in Fig. 12. In this way, since the current flows through the branches the skin effect is minimized.
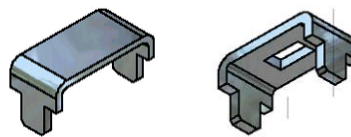
Fig. 12 Rectangular MBB without and with the hole in the middle.

It should be noted that a hollow MBB (see Fig. 12) must be thicker than a same MBB without a hole in order to handle the same current intensity.

To demonstrate the difference between transducers with a circular MBB, a rectangular MBB and a rectangular hollow MBB properly, it is necessary to analyze their frequency responses. In order to do so, the three transducers are realized using all three types of MBBs. The transducer with the circular MBB is shown in Fig. 13.
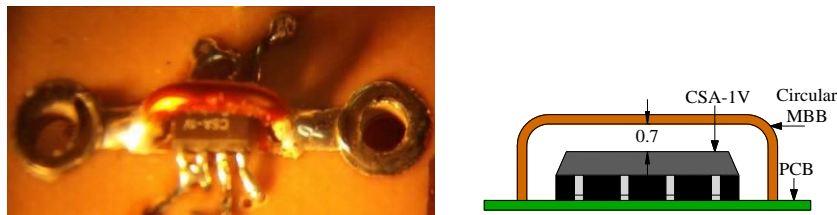
Fig. 13 Transducer with the circular MBB.

The transducer with the rectangular MBB, capable of handling currents up to 50 A, is shown in Fig. 14.
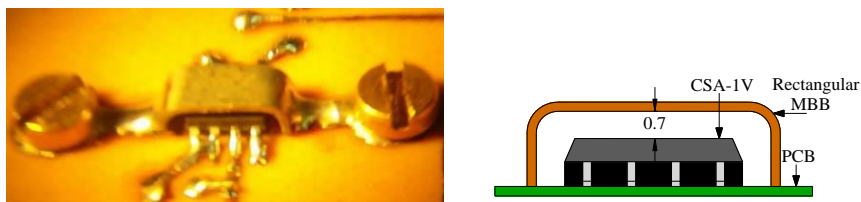
Fig. 14 Transducer with the rectangular MBB.

The transducer with the rectangular hollow MBB is shown in Fig. 15. The MBB is identical to one employed in the transducer shown in Fig. 14 with the only difference being the hole.
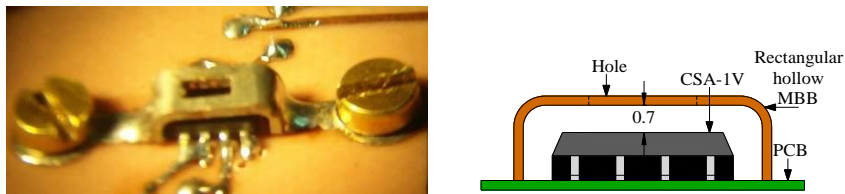
Fig. 15 Transducer with the rectangular hollow MBB.

The frequency responses of all three transducers are shown in Fig. 16. The sensitivity of the transducer with the circular MBB for DC current is S=34 mV/A, the sensitivity of the transducer with the rectangular MBB for DC current is S=35 mV/A while the sensitivity of the transducer with the rectangular hollow MBB for DC current is S=28.36 mV/A.

As can be seen from Fig. 16 the frequency response of the transducer with the circular MBB (see Fig. 13) has the 3 dB sensitivity attenuation (sensitivity is equal to 0.7) at 100 kHz which corresponds to the frequency response of the CSA-1V sensor itself [9]. For the transducer with the rectangular MBB (see Fig. 14), the 3 dB sensitivity attenuation is around 80 kHz. However, for the transducer with the hollow rectangular MBB (see Fig. 15), the 3 dB sensitivity attenuation is around 100 kHz just like for the transducer with the circular MBB. Based on the measurements shown in Fig. 16, the benefit of the hollow rectangular MBB is evident.
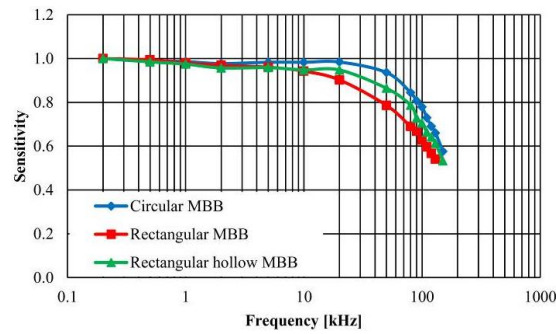
Fig. 16 Frequency responses for all three transducers.

It is possible for a high frequency AC current carrying MBB to be on much higher potential relative to the ground of the CSA-1V. This can lead to the capacitive coupling between the MBB and the CSA-1V. To avoid this, it is necessary to place the electrostatic shield between the MBB and the CSA-1V. Figure 17 shows the electrostatic shield implemented in the transducer with the rectangular hollow MBB. The electrostatic shield is mounted over the top surface of the CSA-1V and soldered on the ground pad on the PCB. The electrostatic shield drops sensitivity and to minimize this it is necessary to employ the electrostatic shield with the shape shown in Fig. 17.
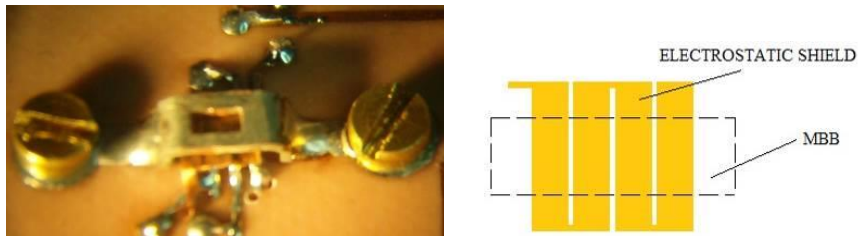
Fig. 17 Transducer with the rectangular hollow MBB and the electrostatic shield.

The frequency response of the transducer with the rectangular hollow MBB and the electrostatic shield is shown in Fig. 18.
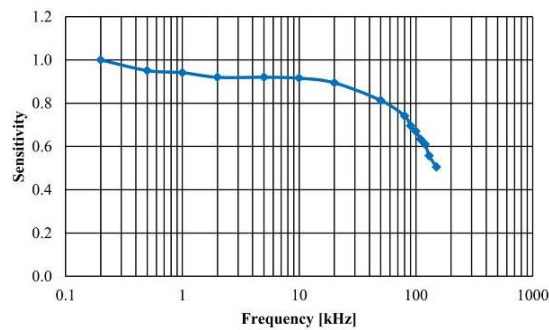
Fig. 18 Frequency response of the transducer with the rectangular hollow MBB and the electrostatic shield.

By comparing the frequency responses for the transducer with and without the electrostatic shield (Fig. 16 and Fig. 18) slight sensitivity decrease is evident.

4.1. MBB transducer with the magnetic shield

To protect the CSA-1V from stray magnetic fields it is possible to employ the magnetic shield shown in Fig. 19. Selection of the shield material must be taken into the account in order not to affect transducer frequency response and linearity [16]. Compared to the magnetic resistance of air, the magnetic resistance of the ferromagnetic shield is practically equal to zero. This means that the magnetic resistance of the magnetic circuit is reduced by factor of two, i.e. the sensitivity is increased by factor of two.
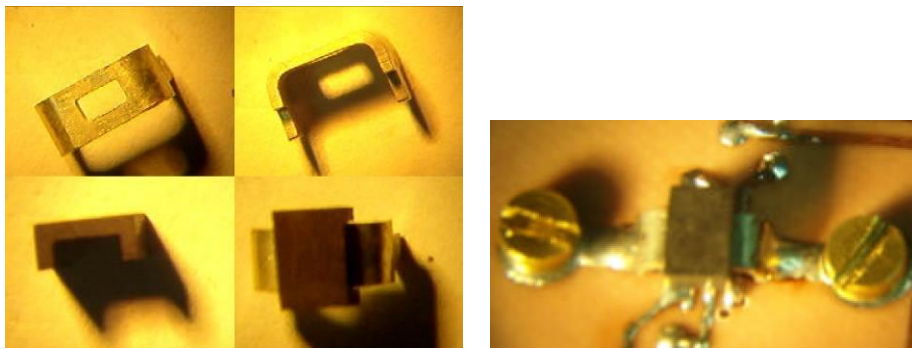
Fig. 19 Magnetic shield structure and transducer with the magnetic shield.

Side effect of the magnetic shield is that it may have hysteresis and a remanence magnetization which can cause offset. The solution to this issue is to insert a layer of Vitrovac beneath the magnetic shield. Vitrovac absorbs the field inflicted by the remanence magnetization. The frequency response of the transducer with the magnetic shield (see Fig. 19) is shown in Fig. 20. Sensitivity for DC current is S=57.8 mV/A.
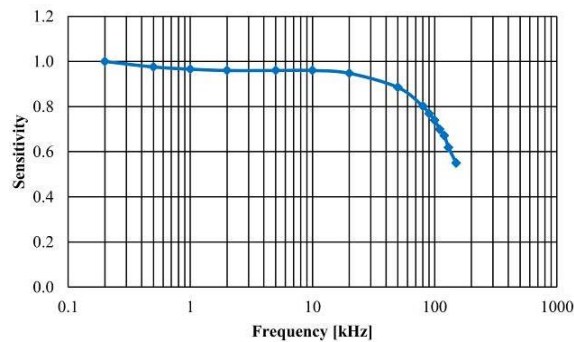
Fig. 20 Frequency response of the transducer with the magnetic shield.

Implementation the magnetic shield does not affect the frequency response which can easily be seen by comparing frequency responses shown in Fig. 16 and Fig. 20.

5. CURRENT TRANSDUCERS BASED ON A BOBBIN COIL

Another method to develop low current transducers based on the CSA-1V is by increasing the magnetic field around the CSA-1V using a multi-turn coil (see Fig. 21). In this way even currents in the order of several tens of miliampers can be accurately measured. During the assembly, the CSA-1V is mounted in a center of a bobbin with the sensing element, inside the CSA-1V, in the middle of a bobbin at equal distance from top and bottom bobbin edge as shown in Fig. 21.
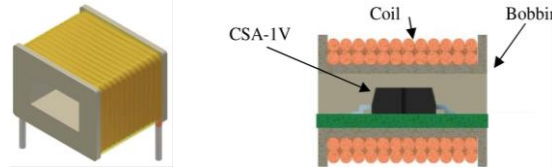
Fig. 21 Multi-turn coil and placment of the CSA-1V inside the bobbin.

Transducer sensitivity is dependent on the coil size and the number of turns. Increased sensitivity and immunity to stray fields can be gained by shielding the coil. The bobbin provides very high dielectric isolation making this a suitable solution for high voltage power supplies with relatively low currents. The output should be scaled to obtain the maximum voltage for the highest current to be measured in order to obtain the best accuracy and resolution.

Based on this method the transducers, capable of measuring currents ranging from 250 mA to 10 A, are produced. Structure of these transducers is the same (see Fig. 22) with the only difference being the type of implemented coil. Depending on the current range there are three types of coil implemented in the transducer:

1. For 250 mA current with 10 V/A sensitivity using 250 turns with AWG34 wire;
2. For 2.5 A current with 1 V/A sensitivity using 24 turns with AWG24 wire;
3. For 10 A current with 0.25 V/A sensitivity using 6 turns of AWG18 wire;
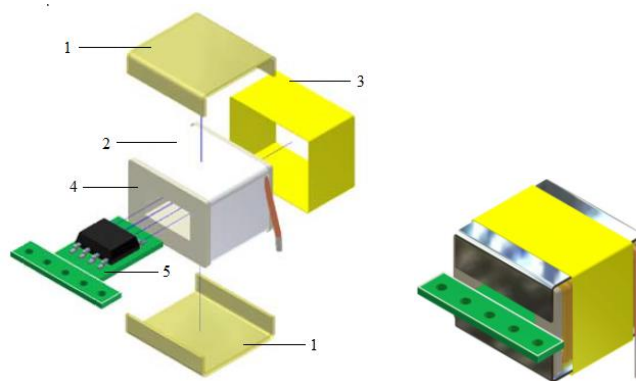
Fig. 22 Transducer structure: 1. shields; 2. duct tape; 3. foil; 4. bobbin; 5. CSA-1V.

Components shown in Fig. 22 are fitted in a cubic box and properly sealed. Photo of the realized transducer is shown in Fig 23.
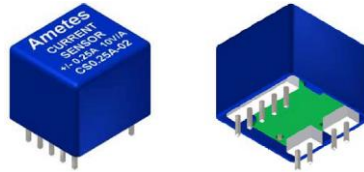
Fig. 23 Photo of the realized transducer.

The transducer can be adjusted to output either a bipolar or unipolar voltage. The transfer functions for both output types are shown in Fig. 24.
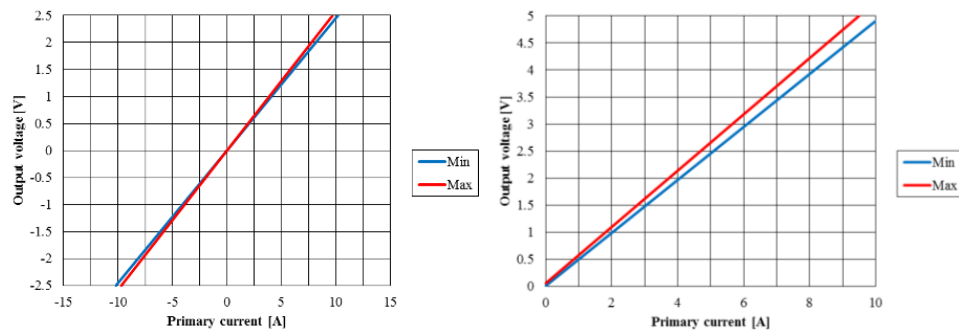
Fig. 24 Transfer function for bipolar and unipolar output.

When a transducer is inserted in a primary circuit its resistance plays an important role because it acts an insertion resistance and can create an undesired voltage drop. For this reason, it is important to keep a transducer resistance as low as possible. The resistances of the realized transducers are 6 Ω for 0.25A, 0.06 Ω for 2.5 A and 0.006 Ω for 10 A.

6. BUS BAR CURRENT TRANSDUCERS

Currents ranging up to few thousands of amperes can be measured in the similar way as presented in previous two methods. In this way, instead of employing a PCB trace or a MBB, the idea is to conduct current trough an electrolytic copper bus bar and to fit the CSA-1V in the middle of a bus bar to measure current. Rather than employing only one CSA-1V effective cancellation of stray fields without magnetic cores or shielding can be achieved by employing two CSA-1Vs. For this reason, the bus bar transducer is realized using the anti-differential configuration of two CSA-1Vs shown in Figs. 8 and 9. Photo of the realized bus bar transducer is shown in Fig 25.

Fig. 25 Copper bus bar.

As stated above, the skin effect within massive rectangular conductors such as the bus bar shown in Fig. 25 can be manifested at very low frequencies in the order of several tens of Hz. The skin effect has a major impact in rectangular bus bars [17, 18] with one of the major issues being a redistribution of the magnetic flux density [19]. For this reason, it is necessary to evaluate transducer under DC and AC current. Frequency and phase measurements are conducted using the DC current source with modulation from 1 Hz to 250 Hz and using the power AC current source. Measurement results are shown in Fig. 26. The blue curve is obtained using the DC source while the red curve is obtained using the AC source. Frequency ranges for both current sources partly overlap.
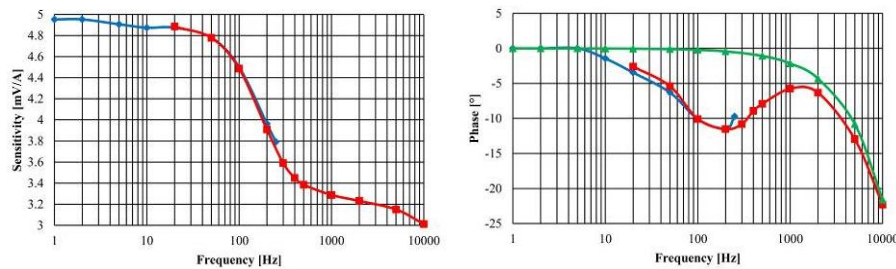
Fig. 26 Frequency and phase responses of the bus bar transducer.

Based on these measurements, it is evident that skin effect becomes significant for frequencies higher than 20 Hz. Therefore, it is unnecessary to use DC current source hence every subsequent measurement is performed using the AC current source.

On the phase response graph (see Fig. 26), the blue curve is obtained using the DC current source, the red curve is obtained using the AC current source while the green curve represents the phase response of the CSA-1V which has a dominant role on high frequencies. The transducer phase response on low frequencies is influenced by the bus bar and surroundings.

Issue with the frequency dependence of the transducer sensitivity can be resolved by implementing at least one of the following methods or by their combination:
1. Unsymmetrical placement of the CSA-1Vs with regard to the bus bar;
2. Application of a magnetic filter;
3. Application of an electronic filter.
4. Cutting out notches in a bus bar in order to produce a restrictive region.

6.1. Unsymmetrical placement of the CSA-1Vs

To evaluate the effect of the CSA-1Vs position on the bus bar, series of measurements are performed in which the both CSA-1Vs are placed at the same distance from the middle of the bus bar as illustrated in Fig. 27.
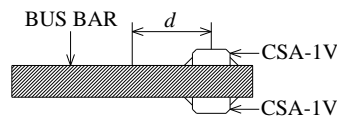
Fig. 27 CSA-1V positions on the bus bar.

Since the skin effect forces current to flow along the outer edges of the bus bar, the idea is to find a suitable position, for the CSA-1Vs to be mounted, at which the field changes originating from current redistribution are the least. The measurement results of this experimentation are shown in Fig. 28.
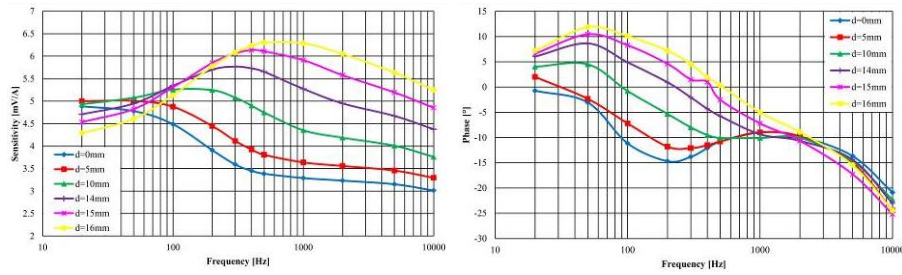
Fig. 28 Frequency and phase responses of the bus bar transducer
with unsymmetrical placement of the CSA-1Vs.

Based on these measurements, the ideal position to mount the CSA-1Vs is where the frequency response is the flattest.

6.2. Magnetic filter

The frequency response can be improved using the passive method based on the assembly of a massive flat conductor above the bus bar and the CSA-1V. This conductor will induce eddy currents which will cancel the primary magnetic field. Consequently, the magnetic field lines will bypass the conductor. Instead, they will concentrate between the bus bar and the conductor mounted above the CSA-1V. Moreover, the current distribution in the bus bar with the conductor mounted above will not be the same as in the case without the conductor, i.e. the current density in the bus bar will be higher on the side closer to the conductor.

To obtain a flat frequency response, the copper magnetic filter is employed in the way shown in Fig. 29.
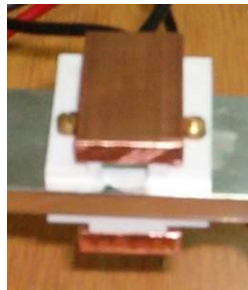
Fig. 29 Application of the magnetic filter on the transducer.

Frequency and phase responses of the bus bar transducer with the magnetic filter (see Fig. 29) are shown in Fig. 30.
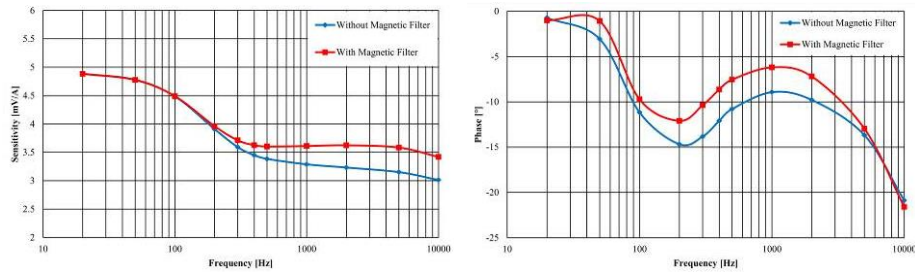
Fig. 30 Frequency and phase responses of the bus bar transducer with the magnetic filter.

Based on the measurements shown in Fig. 30, it is evident that the magnetic filter reduces sensitivity drop caused by the skin effect, i.e. it increases sensitivity. As the sensitivity drop caused by the skin effect is roughly 40%, it is obvious that the magnetic filter reduces the initial impact of the skin effect for 10%. Magnetic filter also improves the phase response.

6.3. Electronic filter

Fig. 31 shows electrical schematic of the bus bar transducer. Summation of outputs from two CSA-1Vs is performed using a differential amplifier AD623 with unity gain.
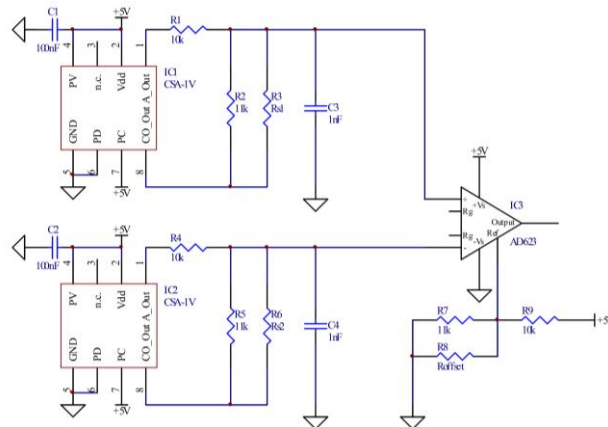
Fig. 31 Schematic of the bus bar transducer.

The idea how to employ an electronic filter to obtain a flatter transducer frequency response is to connect a resistor and capacitor in series instead of a gain defining resistor R_G. The resistor is selected so the amplifiers gain compensates the output signal decrease caused by the skin effect. The capacitor is selected so that its impedance begins to decrease when the skin effect begins to impact, meaning that its impedance is zero when

practically entire current flows along the bus bar outer edges. On this basis, a 220 kΩ resistor and a 2.2 nF capacitor are selected. Frequency and phase responses of the bus bar transducer with the electronic filter are shown in Fig. 32.
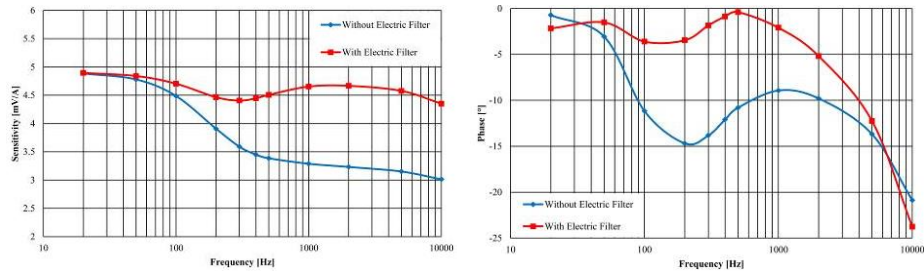
Fig. 32 Frequency and phase responses of the bus bar transducer with the electronic filter.

Based on these measurements it is evident that the electronic filter reduces sensitivity drop at the same time improving the phase response.

6.4. Bus bar with the restrictive region

By having the notches cut out in a bus bar (see Fig. 33) nearly a circular cross section of the restrictive region is obtained. For conductors with a circular cross section, redistribution of a current density does not impact on distribution of a magnetic field around a conductor. In this way the lateral skin effect is minimized.
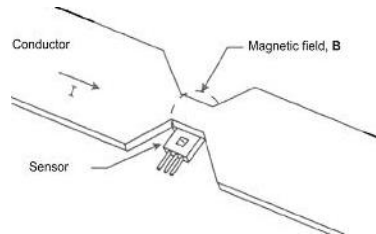
Fig. 33 Bus bar with the restrictive region [20].

Since AC current flows through the restrictive region of the bus bar the magnetic flux density around the restrictive region is greater than around the rest of the bus bar. In addition to this, combination of the anti-differential configuration of Hall effect sensors and a notched bus bar provides the better immunity to stray magnetic fields mainly because Hall effect sensors are close to each other. However, it should be noted that having the notches cut out may cause an overheating at the restrictive region [20].

6.5. Optimized bus bar current transducer

In order to improve the frequency response, i.e. to obtain flat frequency response, the optimized bus bar current transducer comprising top three previously presented methods is realized. The electronic filter is composed of a 330 kΩ resistor and a 2.2 nF capacitor,

the CSA-1Vs are mounted 5 mm away from the middle of the bus bar and the magnetic filter is applied. Overall the obtained amplitude error is less than 1% as shown on Fig. 34.
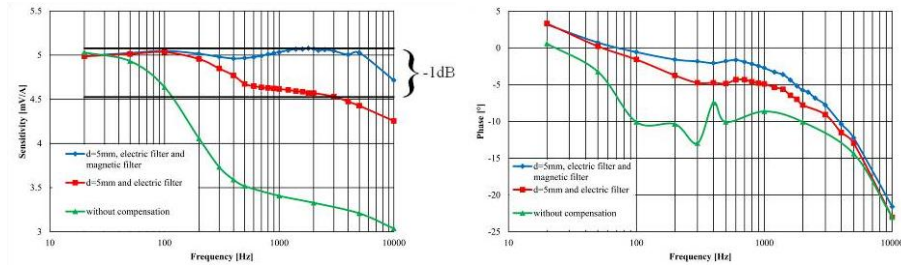
Fig. 34 Frequency and phase responses of the optimized bus bar transducer.

Effect of the applied methods can be easily spotted on the frequency response in Fig. 34 because they result in 55% better frequency response compared to the transducer without compensation.

6.6. Braid bus bar

Another way to minimize the skin effect is rather than to employ plain bus bar to employ a braid bus bar, such as one shown in Fig 35. The application of a braid bus bar, consisted of a thin insulated wires, results in a spatial averaging of a current density so that a distribution of a magnetic field around the conductor is not frequency depended.

Fig. 35 Braid bus bar.

The disadvantage of this solution is that it is not easy to achieve a rigid attachment between a flexible braid and a Hall effect sensor. Movement of a Hall effect sensor relative to a braid bus bar results in a sensitivity change. Therefore, if necessary, this issue must be properly addressed.

6.7. Current transducer with magnetic shielded conductor

The skin effect in rectangular bus bars can be minimized or even eliminated with partial shielding of the bus bar. The idea is to fit ferromagnetic plates, shaped like letter "C", on the side edges of a bus bar as shown in Fig. 36.
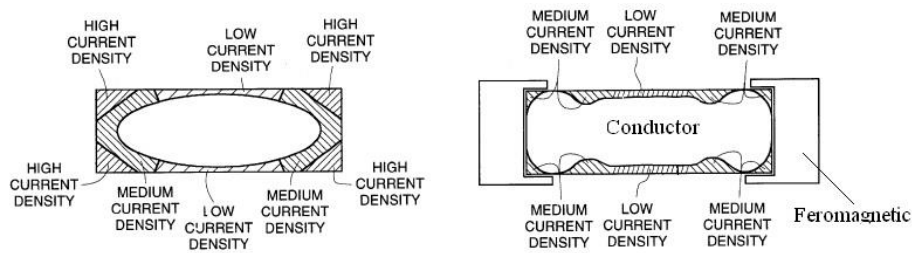
Fig. 36 Partial shielding of the bus bar [21].

Fig. 36 illustrates current density distribution in a bus bar without (left bus bar) and with partial magnetic shield (right bus bar).

This method is presented in patent [21] and discussed in paper [22]. Optimization of size and shape of ferromagnetic shields can result in a significantly better transducer frequency response keeping dimensions of bus bar the same. Minimization of skin effect reduces heating of a bus bar. Magnetic structures presented in [1], [2] also minimize AC resistance, which can be useful for some applications.

7. CONCLUSION

This paper reviews several types of coreless open-loop current transducers based on the Hall effect sensor CSA-1V capable of measuring AC and DC currents ranging from several tens of miliamperes up to several hundreds of amperes. During the development of each transducer special attention was paid on solving problems related to the frequency response. In addition, attention was paid not to disrupt the linearity and to achieve satisfactory immunity to stray magnetic fields.

Another goal of this paper is to expand the scope of use of the realized transducers by providing a lot of useful guidelines for designers faced with the challenges of current measurement using Hall effect sensors.

The first experiments were related to the MBB transducers suitable for current measurements up to several tens of amperes. With MBBs the skin effect becomes noticeable at frequencies greater than 10 kHz. The issue with the skin effect has been overcome by drilling a hole in the bus bar. The issue with stray magnetic fields has been overcome by implementing a ferromagnetic shield and anti-differential configuration of two CSA-1Vs.

The second experiments were related to the transducers based on massive copper bus bars with cross sections which can handle currents up to several hundred of amperes. These solutions employ different ways of position CSA-1Vs relative to the bus bar, the application of magnetic filter and application of electronic filter.

Some of the presented solutions for frequency response improvement are novelty and have never been described in the literature.

REFERENCES

[1] R. S. Popović, *Hall Effect Devices*. Institute of Physics Publishing, Bristol and Philadelphia, 2004.

[2] Honeywell Inc., "Hall Effect Sensing and Application," Micro switch sensing and control, 2002.

[3] D. R. Popović, S. Dimitrijević, M. Blagojević, P. Kejik, E. Schurig, R. S. Popović, "Three-axis teslameter with integrated Hall probe free from the planar Hall effect," In Proc. of the of Instrumentation and Measurement, Technology Conference, Sorrento, Italy, no. 6384, pp. 24-27, 2006.

[4] D. R. Popović, S. Dimitrijević, M. Blagojević, P. Kejik, E. Schurig, R. S.Popović, "Three-axis teslameter with integrated Hall probe," *IEEE Transactions on Instrumentation and Measurement*, vol. 56, issue 4, pp. 1396-1402, 2007.

[5] D. M. Veličković, S. R. Aleksić, "A numerical procedure for solving skin effect integral equation in thin strip conductors," *Facta Universiatis, Series: Electronics and Energetics*, vol. 14, no. 2, pp. 253-270, 2001.

[6] M. Greconici, G. Madescu, M. Mot, "Skin effect analysis in a free space conductor," *Facta Universiatis, Series: Electronics and Energetics*, vol. 23, no. 2, pp. 207-215, 2010.

[7] R. S. Popović, Z. Randjelović, D. Manić, "Integrated Hall-effect magnetic sensors," *Sensors and Actuators A: Physical*, vol. 91, pp. 46 -50, 2001.

[8] R. S. Popović, P. M. Drljača, P. Kejik, "CMOS magnetic sensors with integrated ferromagnetic parts," *Sensors and Actuators A: Physical*, vol. 129, pp. 94-99, 2006.

[9] Sentron, CSA-1V datasheet, 2008.

[10] Sentron, "Current Sensing with the CSA-1V," Application note, 2008.

[11] M. Blagojević, D. Mančić, "Programator strujnih i 2D magnetnih senzora," *In Proc. of the INFOTEH-JAHORINA 2007*, Jahorina, Bosnia and Herzegovina, no. E-VI-10, 2007, in Serbian.

[12] M. Blagojević, S. Dimitrijević, "Programiranje strujnih senzora CSA-1V i statisticka analiza," *In Proc. of the of XIII conference YU INFO 2007*, Kopaonik, Serbia, pp. 11-14, 2007, in Serbian.

[13] M. Blagojević, M. Radmanović, "Uređaj za kalibraciju strujnih senzora," In Proc. of the INFOTEH-JAHORINA 2007, Jahorina, Bosnia and Herzegovina, no. E-VI-11, 2007, in Serbian.

[14] Z. Petrušić, I. Jovanović, Lj. Vračar, D. Mančić, M. Blagojević, "A wirelles solution of measurement-control system for photovoltaic application," In Proc. of the UNITECH'10 International Scientific Conference, Gabrovo, Bulgaria, vol. 1, pp. 114-122, 2010.

[15] M. Blagojević, Z. Petrušić, D. Mančič, M. Radmanović, "Termička analiza strujne sonde bazirane na senzoru CSA-1V," In Proc. of the XIII Međunarodni simpozijum Energetska elektronika Ee 2005, Novi Sad, Serbia, no. T4-4.8, pp. 1-5, 2005, in Serbian.

[16] P. Ripka, "Current sensors using magnetic materials," *Journal of Optoelectronics and Advanced Materials*, vol. 6, no. 2, pp. 587-592, 2004.

[17] V. Belevitch, "The lateral skin effect in a flat conductor," Philips technical rev. 32, pp. 221-231, 1971.

[18] J. Zhou, A. M. Lewis, "Thin-skin electromagnetic fields around a rectangular conductor bar," *Journal of Physics D: Applied Physics*, vol. 27, pp. 419–425, 1994.

[19] I. Popa, A.-I. Dolan, "Numerical modeling of DC busbar contacts," *Facta Universiatis, Series: Electronics and Energetics*, vol. 24, no. 2, pp. 209-219, 2011.

[20] M. Blagojević, D. Mančić, I. Jovanović, Z. Petrušić, "Current ampacity of bus-bar with neck for application in current transducers," In Proc. of the UNITECH'10 International Scientific Conference, Gabrovo, Bulgaria, vol. 1, pp. 123-127, 2010.

[21] J. S. Gallina, M. Brand, "Magnetic structure for minimizing AC resistance in planar rectangular conductors", Patent US6105236A

[22] T. Mizuno, S. Enoki, T. Suzuki, T. Asahina, M. Noda, H. Shinagawa, "Reduction in eddy current loss in conductor using magnetoplated wire," *IEEJ Transactions on Fundamentals and Materials*, vol. 127, no. 10, pp. 611-620, 2007.